neurotoxicity and cognitive impairments in vitro and in vivo (Walsh et al., 2002; Gong et al., 2003; Lesné et al., 2006), and this was also true in humans (Kuo et al., 1996; Shankar et al., 2008; Noguchi et al., 2009). Therefore, the formation and accumulation of Aβ oligomers has been presumed to play a central role in the pathogenesis and clinical symptoms of AD. Aβs are composed of 38–43 amino acid residues and are generated from the amyloid precursor protein (APP) by β- and γ-secretase-mediated sequential cleavages. A number of mutations linked to familial AD in the *APP* gene have been identified. Recently, an atypical early-onset familial AD, caused by an E693Δ mutation of an APP-producing variant Aβ lacking 22nd Glu was discovered in Japan (Tomiyama et al., 2008). This APP-E693Δ mutation presents rare, autosomal-recessive mutations of the *APP* gene related to familial AD. Patients with the mutation show overt early-onset symptoms of AD but lack Aβ deposition, according to positron emission tomography (PET) scan analysis with a [^{11}C] Pittsburgh compound-B (PIB) radioprobe (Tomiyama et al., 2008; Shimada et al., 2011). The 22nd Glu within the Aβ sequence has a destabilizing effect on the formation of oligomeric structures because of the electrostatic repulsion between the adjacent side chain of 22nd Glu (Kassler et al., 2010), and the deletion of the amino acid residue leads to the ready formation of Aβ oligomers in vitro (Nishitsuji et al., 2009). APP-E693Δ transgenic mice show AD-like pathology, including intracellular oligomer accumulation, but lack extracellular amyloid plaque formation (Tomiyama et al., 2010). However, it remains unclear whether Aβ oligomers are accumulated in familial and sporadic AD patient neural cells and how intracellular Aβ oligomers play a pathological role. The compound and/or drugs that might rescue the Aβ oligomer-induced pathological phenotypes are also unclear. Recent developments in induced pluripotent stem cell (iPSC) technology have facilitated the investigation of phenotypes of patient neural cells in vitro and have helped to overcome the lack of success in modeling sporadic AD.

Here, we report the derivation and neuronal and astroglial differentiation of iPSCs from a familial AD patient with an APP-E693Δ mutation, a familial case with another APP mutation, as well as other sporadic cases. Using patient neurons and astrocytes, we addressed the accumulation and possible pathological roles of intracellular Aβ oligomers in familial and sporadic AD. We found that Aβ oligomers were not proteolytically resistant and that docosahexaenoic acid (DHA) treatment attenuated cellular phenotypes of AD neural cells with intracellular Aβ oligomers in both familial and sporadic AD patients.

RESULTS

iPSC Generation and Cortical-Neuronal Differentiation

Dermal fibroblasts were reprogrammed by episomal vectors (Okita et al., 2011). Control iPSC lines from three unrelated individuals, three and two familial AD iPSC lines from patients with E693Δ[AD(APP-E693Δ)] and V717L[AD(APP-V717L)] APP mutations, respectively, and two sporadic iPSC lines (AD3E211 and AD8K213) from two unrelated patients (Figure S1A available online) were generated (Figures 1A, 1B, and S1B–S1H). To characterize cortical neurons derived from the iPSC lines, we established differentiation methods for cortical neurons by modifying previous procedures (Morizane et al., 2011) (Figure S1I). The differentiated cells expressed the cortical neuron subtype markers SATB2 and TBR1 (Figure 1C), and the differentiated neurons were functionally active (Figures S1J and S1K). There was no prominent difference in the differentiation propensity between control and AD neurons (Figures 1D and S1L).

We analyzed the amounts of extra- and intracellular Aβ40 and Aβ42 (Figures 1E and 1F). As expected, both Aβ species were strongly decreased in all cloned AD(APP-E693Δ) neural cells in comparison to those in control neural cells. In familial AD(APP-V717L) neural cells, an increase in the extracellular Aβ42 level and a corresponding decrease in the intracellular Aβ42 level were observed, and the Aβ42/Aβ40 ratio in the culture medium was increased up to 1.5-fold, suggesting that the abnormality of APP metabolism in AD is dependent on the mutation sites in *APP*. Extracellular Aβ levels in sporadic AD neural cells were not changed in comparison to those in control neural cells, but intracellular Aβ in sporadic AD8K213 neural cells apparently decreased (that is, below the detection limit). APP expression levels in the AD(APP-E693Δ) neural cells were lower than in the others, but the levels of α- and β-secretase-mediated APP processing remained unaltered in all neural cells (Figures 1G, S1M, and S1N). Soluble APPβ production was strongly inhibited by treatment with β-secretase inhibitor IV (BSI) (Figure 1G). Aβ levels in the original fibroblasts and iPSC-derived astrocytes, in which APP expression levels were relatively higher than those in neural cells (data not shown), were lower than those of the corresponding neural cells (Figures S1O and S1P).

Intracellular Accumulation of Aβ Oligomers in AD(APP-E693Δ) and in One of the Sporadic AD Neural Cells

Using an immunocytochemical method with the Aβ-oligomer-specific antibody NU1 (Lambert et al., 2007), we investigated whether AD(APP-E693Δ) neural cells harbor Aβ oligomers or not. We found that Aβ oligomers were accumulated as puncta in the neurons of AD(APP-E693Δ) and in one of the sporadic AD cases (Figure 2A). The area of Aβ-oligomer-positive puncta was significantly increased in AD(APP-E693Δ) neuronal cells relative to control neuronal cells (Figure 2B). Dot blot analysis using cell lysates revealed that Aβ oligomers were markedly elevated in the AD(APP-E693Δ) and sporadic AD8K213 neural cells (Figures 2C and 2D), whereas Aβ oligomers were not detected in the culture medium (data not shown). Another antibody against Aβ, 11A1, which detects low-molecular-weight oligomers rather than the Aβ monomer (Murakami et al., 2010), showed results similar to those observed with NU1 (Figures

(*, $p < 0.001$). There are significant differences between dimethyl sulfoxide (DMSO)-control and BSI treatment in each case (*, $p < 0.001$) except that of AD(APP-E693Δ) for Aβ42.
(F) Aβ40 and Aβ42 in cell lysates (intracellular Aβ). N.D., not detected. Data represent mean ± SD (n = 3 per clone).
(G) The amount of soluble APPβ was not altered in control and AD. Data represent mean ± SD (n = 3 per clone).
See also Figure S1.

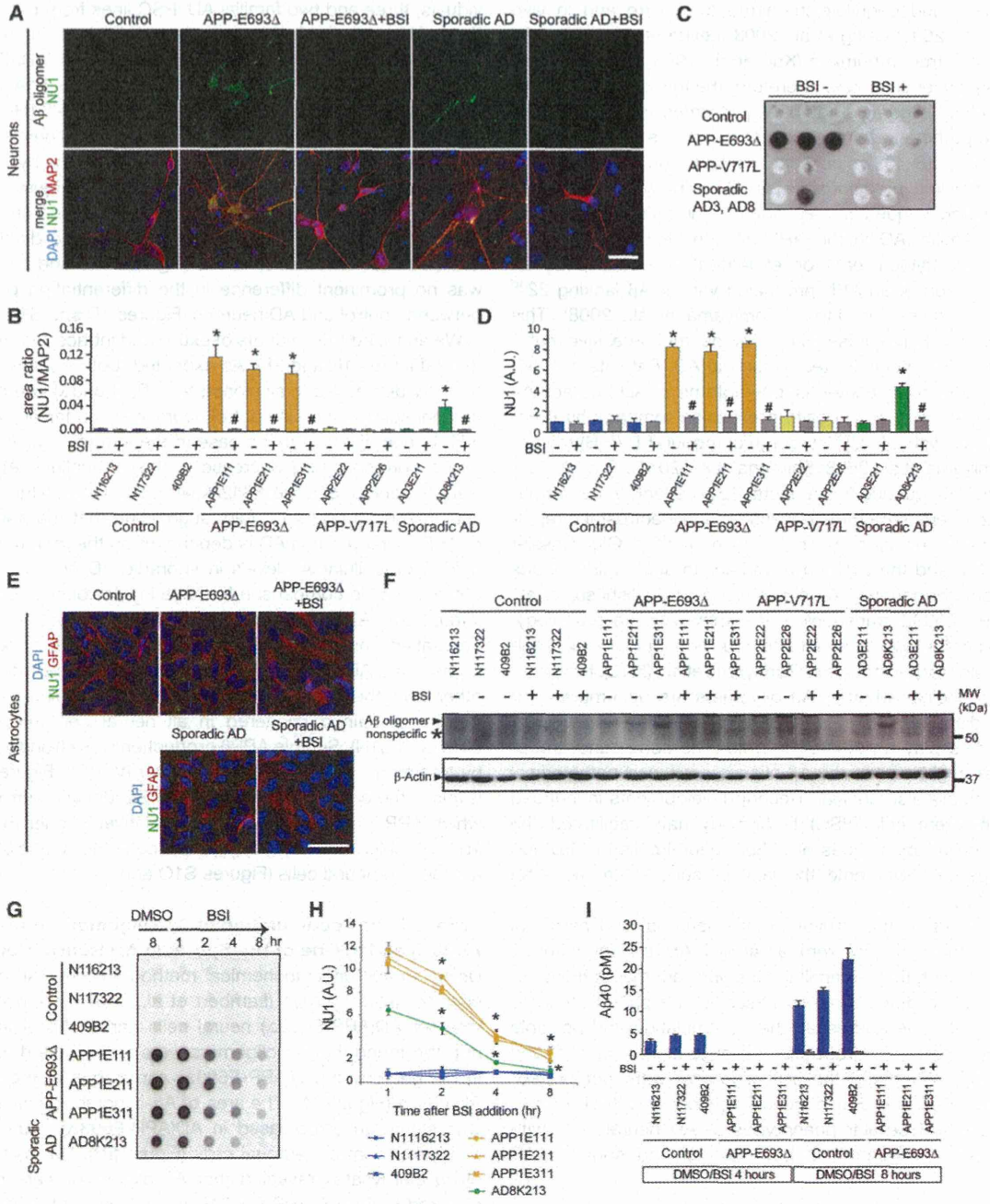

Figure 2. Familial AD(APP-E693Δ) and Sporadic AD iPSC-Derived Neurons Have Intracellular Aβ Oligomers

(A) Intracellular Aβ oligomer accumulation in iPSC-derived neurons (red, MAP2-positive cells) was detected by the Aβ-oligomer-specific monoclonal antibody NU1 (green) with a punctate pattern. Aβ oligomer accumulation was massive in AD(APP-E693Δ) and sporadic AD(AD8K213) neurons but only faint in control neurons. Treatment with 1 μM BSI decreased Aβ oligomer accumulation. DAPI, nuclear staining (blue). The scale bar represents 30 μm.

(B) Quantification of Aβ oligomer accumulation in (A); the ratio of the NU1-positive area in the MAP2-positive area was analyzed. Data represent mean ± SD (n = 3 per clone). Aβ oligomer levels in the AD(APP-E693Δ) and sporadic AD(AD8K213) neural cells without BSI were significantly different from those of other neural cells (*, $p < 0.005$) and from corresponding neural cells with BSI (#, $p < 0.005$).

(C) Dot blot analysis with the use of NU1 antibody. Control (N116213, N117322, 409B2), APP-E693Δ(APP1E111, APP1E211, APP1E211), APP-V717L (APP2E22, APP2E26), and sporadic AD (AD3E211, AD8K213) neural cells were dotted from the left. Blank is RIPA buffer only.

(D) Signals of blot in (C) were quantified. Data represent mean ± SD (n = 3 per clone). Aβ oligomer levels in AD(APP-E693Δ) and sporadic AD(AD8K213) neurons without BSI were significantly different from those of other neurons (*, $p < 0.001$) and from corresponding neurons treated with 1 μM BSI (#, $p < 0.001$).

(E) Aβ oligomer accumulation in AD astrocytes. The scale bar represents 30 μm.

(legend continued on next page)

S2A–S2D). However, Aβ oligomers were not detected in cell lysates from the fibroblasts that generate iPSC lines (Figure S2E). To confirm whether Aβ oligomers were derived from mutant APP(E693Δ), we transduced a lentiviral vector driven by an EF1α promoter to overexpress wild or mutant APP(E693Δ) in control iPSC-derived neural cells and found that Aβ oligomers emerged inside control neural cells overexpressing mutant APP(E693Δ) (Figure S2F).

To investigate the intracellular accumulation of Aβ oligomers in astrocytes derived from control and AD iPSCs, we established an astrocyte-enrichment culture by modifying the method previously reported (Krencik et al., 2011) (Figures S2G–S2J). Dot blot analysis using Aβ oligomer antibodies revealed that the astrocytes of AD(APP-E693Δ) and one of the sporadic AD iPSCs accumulated Aβ oligomers intracellularly (Figures 2E, S2K, and S2L), which was compatible with the results of neurons. On the other hand, we detected no difference in the uptake of extracellular glutamate between control and AD astrocytes (Figure S2M).

Aβ oligomers were also detected as a protein band with a molecular mass of 50~60 kDa by western blot analysis (Figures 2F and S2N). The accumulation of Aβ oligomers was inhibited by treatment with BSI (Figures 2A–2G, S2A–S2D, and S2N). To clarify whether the E693Δ mutation results in accelerated Aβ oligomerization and/or in a proteolytically resistant and stable form of Aβ oligomers, we analyzed the levels of Aβ oligomers over a course of time after BSI treatment. Intracellular Aβ oligomers started to disappear from 2 hr after the treatment with BSI, almost reaching the control level by 8 hr (Figures 2G and 2H). Secretion of Aβ40 from control neural cells was already inhibited at 2 hr after BSI treatment, but the secretion from AD neural cells was under the detection limit in both the presence and absence of BSI (Figure 2I).

Cellular Stress Responses Caused By Intracellular Aβ Oligomers in AD iPSC-Derived Neural Cells

Extracellular Aβ deposition in patient brains carrying APP with an E693Δ mutation is predicted to be extremely low, as amyloid PET imaging with a [^{11}C] PIB probe revealed a far lower signal in the patients than those observed in sporadic AD brains (Tomiyama et al., 2008). Given that processing by β- and γ-secretases largely proceeds within vesicular endosomal compartments, it was possible that Aβ oligomers were associated with specific organelles. We characterized the Aβ oligomer-positive punctate structures in AD(APP-E693Δ) neural cells and astrocytes by coimmunostaining with antibodies for markers of vesicular compartments and subcellular organelles. Subpopulations of Aβ oligomer-positive puncta in the AD neurons showed positive immunostaining for an endoplasmic reticulum (ER) marker, binding immunoglobulin protein (BiP); an early endosomal marker, early endosome-associated antigen-1 (EEA1); and a lysosomal marker, lysosomal-associated marker protein 2 (LAMP2) (data not shown).

To uncover molecules that might be implicated in the dysfunction of AD(APP-E693Δ) neural cells, we analyzed gene expression profiles of control and AD neural cells (Figure 3A and Table S1). Gene ontology analysis revealed that oxidative-stress-related categories, including peroxiredoxin, oxidoreductase, and peroxidase activities, were upregulated in the AD, whereas glycosylation-related categories were downregulated (Figures 3B and 3C and Table S1), suggesting that ER and Golgi function might be perturbed in AD neural cells. Western blot analysis clarified that the amounts of both BiP and cleaved caspase-4 were elevated in the neurons and astrocytes of the AD(APP-E693Δ) case, and that of BiP in one of the sporadic AD cases, AD8K213, but not in fibroblasts (Figures 3D–3F and S3A–S3F). We also found that BSI treatment not only prevented the increase in Aβ oligomer-positive puncta area per cell in the context of AD(APP-E693Δ) lines but also decreased the amount of BiP and cleaved caspase-4 (Figures 3D–3F). *PRDX4*-coding antioxidant protein peroxiredoxin-4 was the most highly upregulated gene (Figure 3C). Western blot analysis confirmed that the amount of peroxiredoxin-4 was increased up to approximately 5- to 7-fold in lysates from AD(APP-E693Δ) and in one of the sporadic AD cases, AD8K213 neural cells, but not in fibroblasts, and was decreased by the BSI treatment (Figures 3D, 3G, S3A, S3D, S3G, and S3H), indicating that the antioxidant stress response was provoked by Aβ oligomer formation in AD(APP-E693Δ) and sporadic AD8K213. To identify pathogenic species evoking oxidative stress in AD(APP-E693Δ), we visualized reactive oxygen species (ROS) and found that ROS was increased in both neurons and astrocytes in AD(APP-E693Δ) and AD8K213 (Figures 3H–3J and S3I –S3L). This increase was counteracted by the BSI treatment. These results indicated that intracellular Aβ oligomers provoked both ER and oxidative stress, and the increase in ROS most likely occurred via a vicious cycle between ER and oxidative stress (Malhotra and Kaufman, 2007).

Alleviation of Intracellular Aβ Oligomer-Induced Cellular Stress by DHA

We evaluated BSI and three additional drugs that had been reported to improve ER stress or to inhibit ROS generation: (1) DHA (Begum et al., 2012), (2) dibenzoylmethane (DBM14-26) (Takano et al., 2007), and (3) NSC23766 (Lee et al., 2002) (Figures 4 and S4). DHA treatment significantly decreased the protein level of BiP, cleaved caspase-4, and peroxiredoxin-4 in AD (APP-E693Δ) neural cells (Figures 4A, 4B, S4A, and S4B), and BiP and peroxiredoxin-4 in sporadic AD8K213 (Figures S4C and S4D). Furthermore, DHA treatment also decreased the generation of ROS in AD(APP-E693Δ) neural cells (Figures 4C and 4D), whereas the amount of Aβ oligomers in cell lysates

(F) Western blot analysis of control and AD neural cells in the presence or absence of BSI. BSI treatment (1 μM) disappeared 6E10-positive ≈55 kDa protein bands in cell lysates of AD(APP-E693Δ) and sporadic AD(AD8K213) neural cells.

(G) Disappearance of Aβ oligomers after BSI treatment was analyzed by dot blot analysis with the use of the NU1 antibody. Intracellular Aβ oligomers started to disappear 2 hr after BSI treatment.

(H) Signals of blots in (G) were quantified. Data represent mean ± SD (n = 3 per clone). BSI treatment (1 μM) decreased intracellular Aβ in AD neural cells and was reduced to 16~23% of vehicle control by 8 hr. Post hoc analysis revealed that the amounts of Aβ oligomers at 2 hr after BSI treatment were significantly decreased in comparison to those of DMSO control oligomers (*, $p < 0.005$).

(I) Changes in extracellular Aβ40 levels were analyzed in the experimental condition of (G). Data represent mean ± SD (n = 3 per clone).

See also Figure S2.

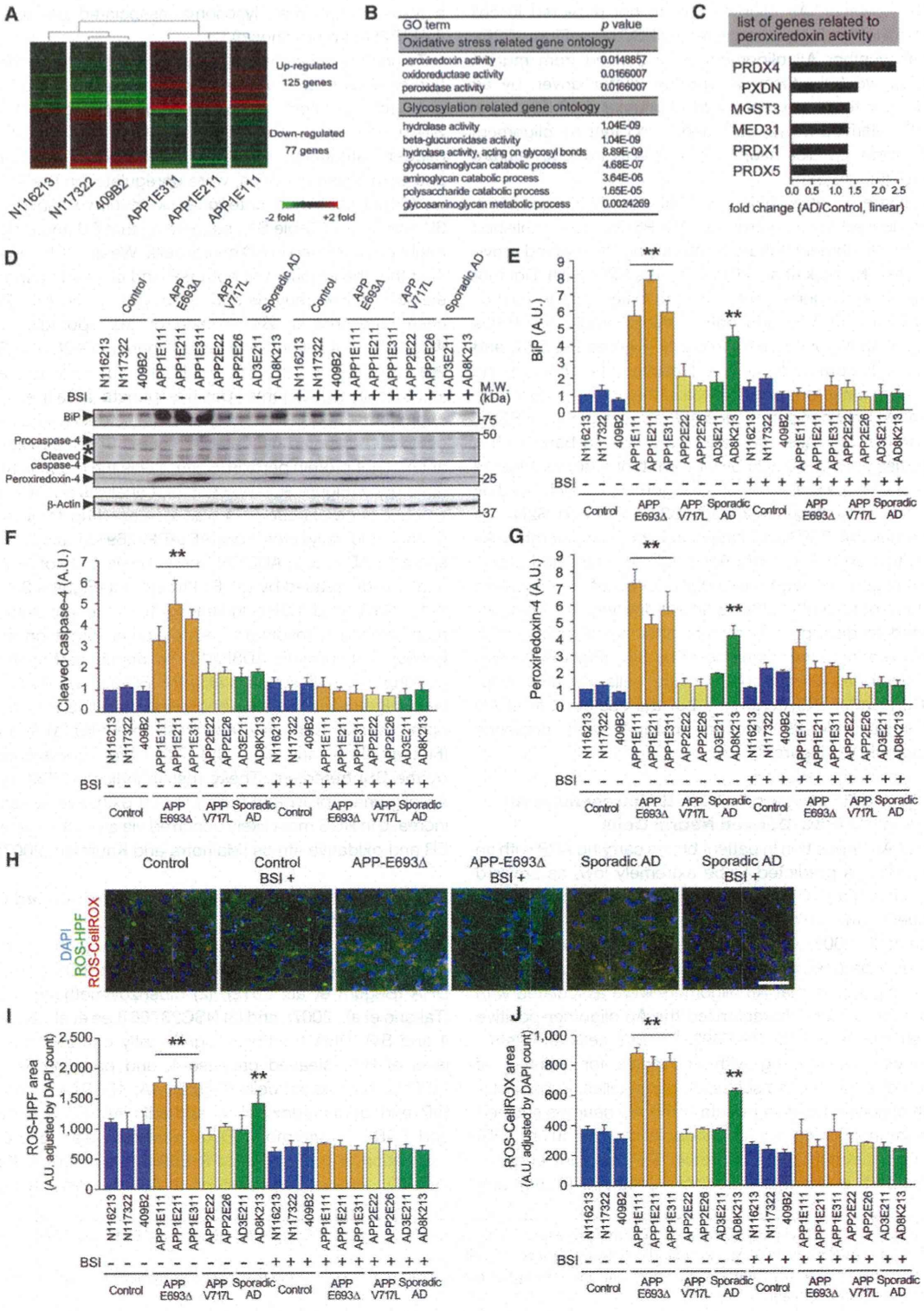

Figure 3. Cellular Stress Responses Caused by Intracellular Aβ Oligomers in Familial AD(APP-E693Δ) and Sporadic AD(AD8K213) iPSC-Derived Neural Cells

(A) Hierarchical clustering analysis of differentiated neuronal cells and a heatmap of significantly up- and downregulated genes in AD neural cells. The statistically significant cutoff p value is < 0.05.

(legend continued on next page)

was not altered (Figures S4E–S4G). In contrast, the high concentration of DHA, DBM14-26, or NSC23766 treatment increased the protein level of BiP (Figure S4B). Finally, to confirm the protective effects of DHA in short-term screening, we analyzed the effect on the survival of AD(APP-E693Δ) neural cells. Neuronal cells were labeled with a lentiviral vector expressing synapsin I-promoter-driven EGFP and cultivated in the medium depleted of neurotrophic factors and neural culture supplements mix. The real-time survival rate of AD(APP-E693Δ) neurons was lower than that of normal control neurons; however, DHA treatment for 16 days partially rescued AD(APP-E693Δ) cell viability (Figures 4E–4G). The real-time survival rate of sporadic AD(AD3E211, AD8K213) neurons for 16 days was unchanged (Figures 4E and 4F and Table S2). We confirmed these results through a lactate dehydrogenase (LDH) assay (Figure 4G). The AD(APP-E693Δ) neurons were also vulnerable to oxidative stress by hydrogen peroxide treatment (Figure S4H). Extracellular Aβ levels were not altered in the assay (Figure 4H).

DISCUSSION

The present study shows that neural cells derived from a patient carrying the pathogenic APP-E693Δ mutation and a sporadic AD patient produce intracellular Aβ oligomers, and the use of these neural cells provided an experimental system for addressing whether such oligomers would cause cellular stress and the killing of neurons and how such intracellular Aβ oligomers might contribute to the disease pathogenesis, despite only one patient carrying the E693Δ mutation being available. Our findings also suggest that the possible heterogeneity of familial and sporadic AD stems from phenotypic differences of intracellular Aβ oligomers and suggests the possibility that DHA, a drug that failed in some clinical trials of AD treatment, might be effective in a portion of AD patients.

We demonstrated that Aβ oligomers were formed and accumulated inside AD(APP-E693Δ) and sporadic AD(AD8K213) neurons by immunostaining (Figures 2A and 2B), dot blot analysis (Figures 2C and 2D), and western blot analysis (Figures 2F and S2N). In addition, intracellular accumulation of Aβ oligomers, which has been supposed to be proteolytically resistant, disappeared after treatment with BSI in both AD neurons (Figures 2G and 2H), indicating that AD(APP-E693Δ) and sporadic AD(AD8K213) neurons still seemed to retain a degrading activity toward Aβ oligomers in which proteasomes, autophagosomes, and/or lysosomes may be involved and, thereby, that the pathological property of Aβ oligomers in a part of AD might be completely abrogated. The sporadic AD(AD8K213) neurons may retain a specific cellular environment that permits the formation of Aβ oligomers. Additional studies aimed at identifying the factors causing such an environment are needed.

We observed that the accumulation of Aβ oligomers induced ER and oxidative stress both in AD(APP-E693Δ) and in sporadic AD(AD8K213) neurons, although caspase-4 activation appeared not to accompany sporadic AD, probably because of the lesser extent of ER stress in comparison to AD(APP-E693Δ). Previously, Nishitsuji et al. (2009) reported that accumulated Aβ oligomers in ER provoke ER stress. This result suggests that oligomers represent a self-aggregating state of Aβ. During this process, Aβ generates ROS, which is supported by the fact that Aβ coordinates the metal ions zinc, iron, and copper, which induce the oligomerization of Aβ. Iron and copper then cause the generation of toxic ROS and calcium dysregulation (Barnham et al., 2004), leading to membrane lipid peroxidation and the impairment of the function of a range of membrane-associated proteins (Hensley et al., 1994; Butterfield, 2003), antioxidant factors being thought to protect ER-stress-induced cellular toxicities (Malhotra and Kaufman, 2007).

We found that intracellular Aβ oligomers were accumulated not only in a case of familial AD with APP-E693Δ mutation but also in a sporadic AD case, although only three clones derived from one familial AD patient carrying an APP-E693Δ mutation and two clones from two sporadic AD patients were analyzed in this study because of the limited number of patients. In contrast, in familial AD with the APP-V717L mutation, of which only one case was available, intracellular Aβ oligomers were not detected, but the extracellular Aβ42/Aβ40 ratio, which is increased in mutant presenilin-mediated familial AD, as reported previously (Yagi et al., 2011), was increased, lending support to the notion that AD could be classified into two categories: extracellular Aβ type and intracellular Aβ type. Although it has been supposed that environmental factors and/or the aging process contribute to neurodegenerative diseases, our findings support the idea that a genetic factor might play a role in a part of sporadic AD, a finding that is compatible with a previous report (Israel et al., 2012). However, identifying the genetic factor would require a larger sample size. The sporadic AD case with intracellular Aβ oligomers might correspond to the case without extracellular Aβ40 elevation of Israel et al. (2012). Analysis of neurons

(B) The gene ontology (GO) term list, calculated from the significantly altered gene expression patterns in the microarray analysis of AD versus control neural cells.
(C) Altered expression levels of genes related to peroxidation activity detected by GO analysis. All values were significantly different from that of the control ($p < 0.05$).
(D–G) Western blot analysis of ER stress markers (BiP and casapase-4), peroxiredoxin-4, and a reference protein (β-actin) in the presence or absence of BSI. (E–G) Densitometric analysis of (D) are shown. Measured values of proteins were normalized by β-actin. Data represent mean ± SD (n = 3 per clone). Levels of BiP (E), cleaved caspase-4 (F), and peroxiredoxin-4 (G) in AD(APP-E693Δ) and sporadic AD(AD8K213) neural cells without BSI were significantly different from those of the other neural cells (**, $p < 0.005$).
(H) Typical images of reactive oxygen species (ROS) staining, detected by HPF or CellROX, in control and AD neural cells with or without BSI treatment. Scale bars represent 30 μm.
(I and J) Quantitative data of (H), ROS-HPF (I), and ROS-CellROX (J). Each value was shown as a ratio of the HPF-stained or CellROX area (average of random 25 fields per sample) adjusted with DAPI counts. Data represent mean ± SD (n = 3 per clone). ROS-generation levels in AD(APP-E693Δ) and sporadic AD(AD8K213) neural cells were significantly different from those of the others (**, $p < 0.001$). Data represent mean ± SD (n = 3 per clone).
See also Figure S3 and Table S1.

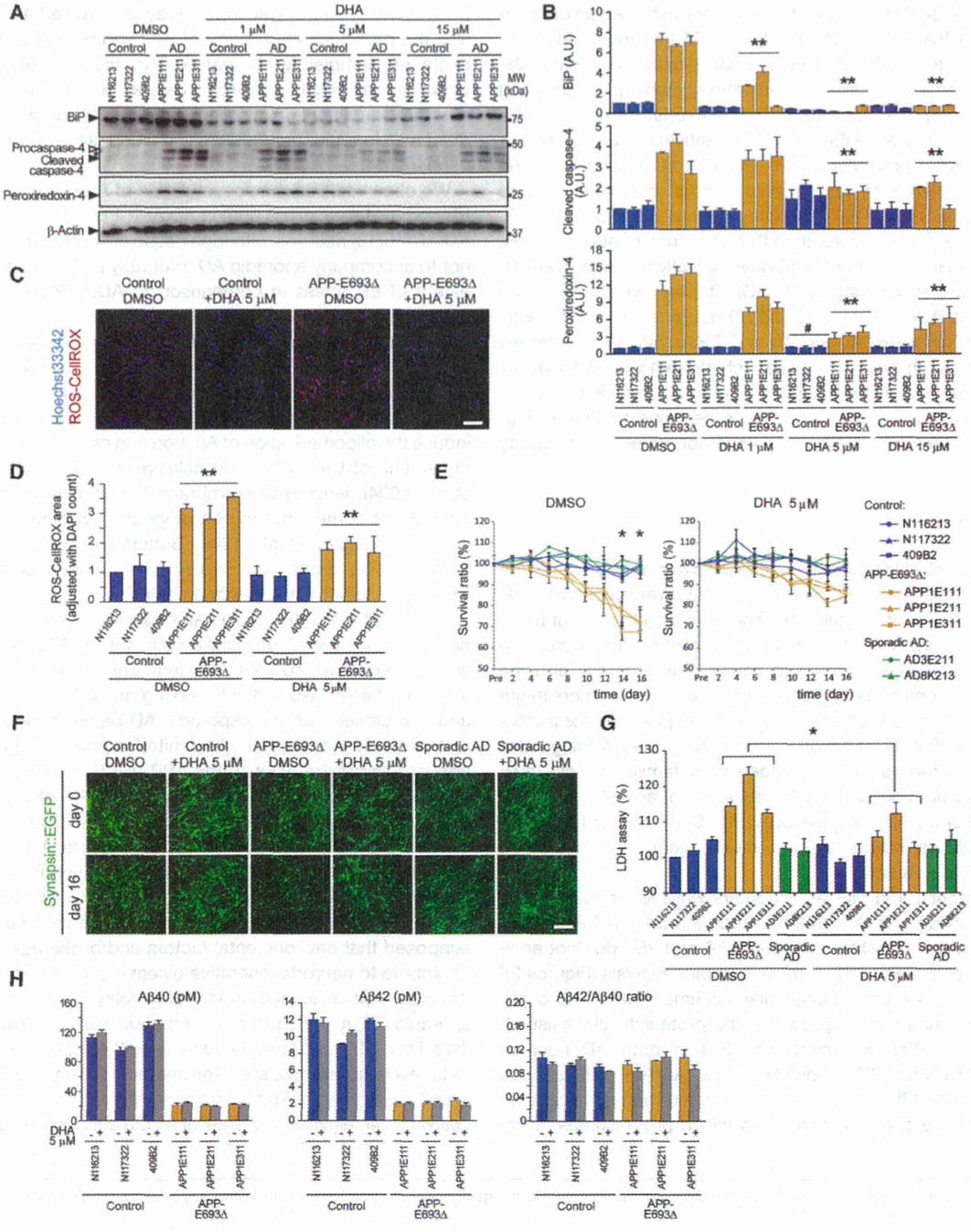

Figure 4. DHA-Alleviated Cellular Stress Caused By Intracellular Aβ Oligomers

(A) Control and AD(APP-E693Δ) neural cells at day 72 were treated with DHA for 48 hr. Then, cells were lysed and subjected to immunoblot analysis (1 μM, 5 μM, and 15 μM of docosahexaenoic acid [DHA]).

(B) Densitometric analysis of (A) is shown. Measured values were normalized by that of β-actin. Data represent mean ± SD (n = 3 per clone). Two-way analysis of variance (ANOVA) showed significant main effects of DHA treatment (BIP, $F_{[3,64]} = 136.712$, $p < 0.001$; cleaved caspase-4, $F_{[3,64]} = 50.855$, $p < 0.001$) with a significant interaction between APP mutation and DHA treatment (BIP, $F_{[3,64]} = 99.658$, $p < 0.001$; cleaved caspase-4, $F_{[3,64]} = 53.005$, $p < 0.001$). Post hoc analysis revealed significant differences between DMSO (control) and DHA treatment (1, 5, and 15 μM) in AD(APP-E693Δ) neural cells (**, $p < 0.001$). Two-way ANOVA for peroxiredoxin-4 showed significant main effects of DHA treatment ($F_{[3,64]} = 16.995$; $p < 0.001$) with a significant interaction between APP mutation and DHA treatment ($F_{[3,64]} = 32.093$; $p < 0.001$). Post hoc analysis revealed significant differences between DMSO-control and DHA treatment (5 and 15 μM) in AD(APP-E693Δ) neural cells (**, $p < 0.001$). In control neural cells, the 5 μM DHA group was significantly different from the other groups (#, $p < 0.005$).

(C) Typical images of ROS-CellROX and Hoechst33342 signals after treatment with vehicle or 5 μM DHA. The scale bar represents 50 μm.

(legend continued on next page)

and astrocytes, as we performed here, from larger numbers of patients might result in the classification of sporadic AD.

To date, the clinical effectiveness of DHA treatment is still controversial (Freund-Levi et al., 2006; Quinn et al., 2010). It is of particular interest that one of two sporadic AD neurons accumulated intracellular Aβ oligomers and showed cellular phenotypes that could respond to DHA but the other did not, and this result may explain why DHA treatment was effective for some AD patients, those with the intracellular Aβ oligomer-associated type of AD, although the timing (that is, the stage of disease development) for starting the treatment would be another critical factor. These results may suggest that patient-specific iPSCs provide a chance to re-evaluate the effect of a drug that failed in AD clinical trials, depending on the selection of the patient type. In the present study, the amount of Aβ oligomers in our culture was not affected by DHA, although it would be effective for reducing cellular stresses, and reducing the oligomerization of Aβ was also presumed to be a candidate mechanism of DHA treatment (Cole and Frautschy, 2006). These results indicate that therapy with DHA would alleviate symptoms. Furthermore, the data showing that BSI treatment leads to a reduction in ROS formation at a relatively similar level (Figure 2G) in both AD and control cells might indicate an Aβ oligomer-independent effect, in addition to an Aβ oligomer-dependent effect, of BSI.

In any event, patient-specific iPSCs would provide disease pathogenesis, irrespective of the disease being in a familial or sporadic form, as well as enable the evaluation of drug and patient classification of AD.

EXPERIMENTAL PROCEDURES

Derivation of Patient-Specific Fibroblasts

Control and AD-derived human dermal fibroblasts (HDFs) were generated from explants of 3 mm dermal biopsies. After 1–2 weeks, fibroblast outgrowths from the explants were passaged.

iPSC Generation

Human complementary DNAs for reprogramming factors were transduced in HDFs with episomal vectors (*SOX2, KLF4, OCT4, L-MYC, LIN28*, and small hairpin RNA for p53). Several days after transduction, fibroblasts were harvested and replated on an SNL feeder cell layer. On the following day, the medium was changed to a primate embryonic stem cell medium (ReproCELL, Japan) supplemented with 4 ng/ml basic FGF (Wako Pure Chemicals Industries, Japan). The medium was changed every other day. iPSC colonies were picked up 30 days after transduction.

Statistical Analysis

All data are shown as mean ± SD. For comparisons of the mean between two groups, statistical analysis was performed by applying Student's t tests after confirming equality between the variances of the groups. When the variances were unequal, Mann-Whitney U tests were performed (SigmaPlot 11.2.0, Systat Software, USA). Comparisons of the mean among three groups or more were performed by one-way, two-way, or three-way analysis of variance followed by a post hoc test with the use of Student-Newman-Keuls Method (SigmaPlot 11.2.0). p values < 0.05 were considered significant.

ACCESSION NUMBERS

The Gene Expression Omnibus accession numbers for microarray data reported in this paper are GSE43326 (gene-expression comparison between control and AD clones), GSE43382 (gene-expression change along with the astroglial differentiation), and GSE43328 (gene-expression comparison of generated iPSCs).

SUPPLEMENTAL INFORMATION

Supplemental Information contains Supplemental Experimental Procedures, four figures, and two tables and can be found with this article online at http://dx.doi.org/10.1016/j.stem.2013.01.009.

ACKNOWLEDGMENTS

We would like to express our sincere gratitude to all our coworkers and collaborators, Mari Ohnuki, Megumi Kumazaki, Mitsuyo Kawada, Fumihiko Adachi, Takako Enami, and Misato Funayama for technical assistance; Nobuya Inagaki and Norio Harada for technical advice; and Kazumi Murai for editing the manuscript. This research was funded in part by a grant from the Funding Program for World-Leading Innovative R&D on Science and Technology (FIRST Program) of the Japan Society for the Promotion of Science (JSPS) to S.Y., from the Alzheimer's Association (IIRG-09-132098) to H.M., from the JST Yamanaka iPS Cell Special Project to S.Y. and H.I., from CREST to H.I., H.M., N.I., and T.T., from a Grant-in-Aid from the Ministry of Health, Labour and Welfare of Japan to H.I., from a Grant-in-Aid for Scientific Research on Innovative Area "Foundation of Synapse and Neurocircuit Pathology" (22110007) from the Ministry of Education, Culture, Sports, Science and Technology of Japan to H.I. and N.I., and from the Japan Research Foundation for Clinical Pharmacology to H.I. H.I. conceived the project; T.K., N.I., M.A., and H.I. designed the experiments; T.K., N.I., M.A., K.W., C.K., R.N., N.E., N.Y. and K. Tsukita performed the experiments; T.K., N.I., M.A., and H.I. analyzed the data; K.O., I.A., K.M., T.N., K.I., W.L.K., O.H., S.H., and T.C. contributed

(D) Quantitative data of (C) is shown. Each value indicated the ratio of the CellROX-stained area (an average of random 25 fields per sample) adjusted with DAPI counts. Data represent mean ± SD (n = 3 per clone). Two-way ANOVA showed significant main effects of DHA treatment ($F_{[1,32]} = 43.140$; $p < 0.001$) with a significant interaction between the APP mutation and DHA treatment ($F_{[3,32]} = 23.410$; $p < 0.001$). The DHA group in AD(APP-E693Δ) neural cells was significantly different from the other groups (**, $p < 0.005$).

(E) Real-time survival rate of control and AD neural cells with and without DHA showing cell viability. The numbers of control and AD(APP-E693Δ) neurons with Synapsin I-promoter-driven EGFP were sequentially imaged (average of 25 random fields per sample) and counted to assess the survival ratio (n = 3 per clone). Data represent mean ± SD (n = 3 per clone). In the cell-survival ratio, three-way ANOVA showed significant main effects of the APP mutation ($F_{[1,256]} = 377.611$; $p < 0.001$), DHA treatment ($F_{[1,256]} = 36.117$; $p < 0.001$), and time ($F_{[7,256]} = 65.272$; $p < 0.001$), with significant interactions between the APP mutation and DHA treatment ($F_{[1,256]} = 18.315$; $p < 0.001$), between the APP mutation and time ($F_{[7,256]} = 20.023$; $p < 0.001$), between DHA treatment and time ($F_{[7,256]} = 4.534$; $p < 0.001$), and among all three factors ($F_{[7,256]} = 5.277$; $p < 0.001$). Post hoc analysis revealed that, on day 14 and day 16, AD(APP-E693Δ) neural cells were more vulnerable in the long culture than control neural cells and that DHA treatment rescued the vulnerability (*, $p < 0.001$).

(F) Typical images of Synapsin::EGFP neurons used in real-time survival assay. The scale bar represents 50 μm.

(G) Cytotoxicity in neural culture derived from control and AD iPSCs after treatment with DHA (5 μM) for 16 days. Measured fluorescent lactate dehydrogenase (LDH) release served as a measure of cytotoxicity. Data represent mean ± SD (n = 3 per clone). Two-way ANOVA showed significant main effects of DHA treatment ($F_{[1,32]} = 16.710$; $p < 0.001$) with a significant interaction between APP-E693Δ mutation and DHA treatment ($F_{[3,32]} = 9.210$; $p < 0.005$). There was a significant difference in AD(APP-E693Δ) neural cells between the DMSO-control and DHA groups (*, $p < 0.05$).

(H) Aβ40 and Aβ42 secreted from iPSC-derived neurons into medium (extracellular Aβ) at day 16 of the long-term culture were measured at 48 hr after the last medium change. Data represent mean ± SD (n = 3 per clone).

See also Figure S4 and Table S2.

reagents, materials and analysis tools; Y.K., Y.O., Y.S., M.N., K.Y., S.Y., S.S., T.A., R.H., and S.U. recruited the patients; R.T., H.M., and S.Y. provided critical reading and scientific discussions; T.S., K.K., T.T., and K. Takahashi performed microarray analysis; T.A. performed karyotyping; A.W. performed bisulfite genomic sequencing; K.I. and D.W. performed electrophysiology; K. Tsukita, T.K., and H.H. produced the lentivirus; H.I., N.I., M.A., and T.K. wrote the paper. The experimental protocols dealing with human or animal subjects were approved by the institutional review board at each institute. S.Y. is a member without salary of the scientific advisory boards of iPierian, iPS Academia Japan, Megakaryon Corporation, and Retina Institute Japan.

Received: February 27, 2012
Revised: December 22, 2012
Accepted: January 18, 2013
Published: February 21, 2013

REFERENCES

Barnham, K.J., Masters, C.L., and Bush, A.I. (2004). Neurodegenerative diseases and oxidative stress. Nat. Rev. Drug Discov. *3*, 205–214.

Begum, G., Kintner, D., Liu, Y., Cramer, S.W., and Sun, D. (2012). DHA inhibits ER Ca^{2+} release and ER stress in astrocytes following in vitro ischemia. J. Neurochem. *120*, 622–630.

Butterfield, D.A. (2003). Amyloid β-peptide [1-42]-associated free radical-induced oxidative stress and neurodegeneration in Alzheimer's disease brain: mechanisms and consequences. Curr. Med. Chem. *10*, 2651–2659.

Cole, G.M., and Frautschy, S.A. (2006). Docosahexaenoic acid protects from amyloid and dendritic pathology in an Alzheimer's disease mouse model. Nutr. Health *18*, 249–259.

Freund-Levi, Y., Eriksdotter-Jönhagen, M., Cederholm, T., Basun, H., Faxén-Irving, G., Garlind, A., Vedin, I., Vessby, B., Wahlund, L.O., and Palmblad, J. (2006). Omega-3 fatty acid treatment in 174 patients with mild to moderate Alzheimer disease: OmegAD study: a randomized double-blind trial. Arch. Neurol. *63*, 1402–1408.

Gong, Y., Chang, L., Viola, K.L., Lacor, P.N., Lambert, M.P., Finch, C.E., Krafft, G.A., and Klein, W.L. (2003). Alzheimer's disease-affected brain: presence of oligomeric A β ligands (ADDLs) suggests a molecular basis for reversible memory loss. Proc. Natl. Acad. Sci. USA *100*, 10417–10422.

Haass, C., and Selkoe, D.J. (2007). Soluble protein oligomers in neurodegeneration: lessons from the Alzheimer's amyloid β-peptide. Nat. Rev. Mol. Cell Biol. *8*, 101–112.

Hensley, K., Carney, J.M., Mattson, M.P., Aksenova, M., Harris, M., Wu, J.F., Floyd, R.A., and Butterfield, D.A. (1994). A model for β-amyloid aggregation and neurotoxicity based on free radical generation by the peptide: relevance to Alzheimer disease. Proc. Natl. Acad. Sci. USA *91*, 3270–3274.

Israel, M.A., Yuan, S.H., Bardy, C., Reyna, S.M., Mu, Y., Herrera, C., Hefferan, M.P., Van Gorp, S., Nazor, K.L., Boscolo, F.S., et al. (2012). Probing sporadic and familial Alzheimer's disease using induced pluripotent stem cells. Nature *482*, 216–220.

Kassler, K., Horn, A.H., and Sticht, H. (2010). Effect of pathogenic mutations on the structure and dynamics of Alzheimer's A β 42-amyloid oligomers. J. Mol. Model. *16*, 1011–1020.

Krafft, G.A., and Klein, W.L. (2010). ADDLs and the signaling web that leads to Alzheimer's disease. Neuropharmacology *59*, 230–242.

Krencik, R., Weick, J.P., Liu, Y., Zhang, Z.J., and Zhang, S.C. (2011). Specification of transplantable astroglial subtypes from human pluripotent stem cells. Nat. Biotechnol. *29*, 528–534.

Kuo, Y.M., Emmerling, M.R., Vigo-Pelfrey, C., Kasunic, T.C., Kirkpatrick, J.B., Murdoch, G.H., Ball, M.J., and Roher, A.E. (1996). Water-soluble Abeta (N-40, N-42) oligomers in normal and Alzheimer disease brains. J. Biol. Chem. *271*, 4077–4081.

Lambert, M.P., Velasco, P.T., Chang, L., Viola, K.L., Fernandez, S., Lacor, P.N., Khuon, D., Gong, Y., Bigio, E.H., Shaw, P., et al. (2007). Monoclonal antibodies that target pathological assemblies of Abeta. J. Neurochem. *100*, 23–35.

Lee, M., You, H.J., Cho, S.H., Woo, C.H., Yoo, M.H., Joe, E.H., and Kim, J.H. (2002). Implication of the small GTPase Rac1 in the generation of reactive oxygen species in response to β-amyloid in C6 astroglioma cells. Biochem. J. *366*, 937–943.

Lesné, S., Koh, M.T., Kotilinek, L., Kayed, R., Glabe, C.G., Yang, A., Gallagher, M., and Ashe, K.H. (2006). A specific amyloid-β protein assembly in the brain impairs memory. Nature *440*, 352–357.

Malhotra, J.D., and Kaufman, R.J. (2007). Endoplasmic reticulum stress and oxidative stress: a vicious cycle or a double-edged sword? Antioxid. Redox Signal. *9*, 2277–2293.

Morizane, A., Doi, D., Kikuchi, T., Nishimura, K., and Takahashi, J. (2011). Small-molecule inhibitors of bone morphogenic protein and activin/nodal signals promote highly efficient neural induction from human pluripotent stem cells. J. Neurosci. Res. *89*, 117–126.

Murakami, K., Horikoshi-Sakuraba, Y., Murata, N., Noda, Y., Masuda, Y., Kinoshita, N., Hatsuta, H., Murayama, S., Shirasawa, T., Shimizu, T., and Irie, K. (2010). Monoclonal antibody against the turn of the 42-residue amyloid β-protein at positions 22 and 23. ACS Chem. Neurosci. *1*, 747–756.

Nishitsuji, K., Tomiyama, T., Ishibashi, K., Ito, K., Teraoka, R., Lambert, M.P., Klein, W.L., and Mori, H. (2009). The E693Δ mutation in amyloid precursor protein increases intracellular accumulation of amyloid β oligomers and causes endoplasmic reticulum stress-induced apoptosis in cultured cells. Am. J. Pathol. *174*, 957–969.

Noguchi, A., Matsumura, S., Dezawa, M., Tada, M., Yanazawa, M., Ito, A., Akioka, M., Kikuchi, S., Sato, M., Ideno, S., et al. (2009). Isolation and characterization of patient-derived, toxic, high mass amyloid β-protein (Abeta) assembly from Alzheimer disease brains. J. Biol. Chem. *284*, 32895–32905.

Okita, K., Matsumura, Y., Sato, Y., Okada, A., Morizane, A., Okamoto, S., Hong, H., Nakagawa, M., Tanabe, K., Tezuka, K., et al. (2011). A more efficient method to generate integration-free human iPS cells. Nat. Methods *8*, 409–412.

Quinn, J.F., Raman, R., Thomas, R.G., Yurko-Mauro, K., Nelson, E.B., Van Dyck, C., Galvin, J.E., Emond, J., Jack, C.R., Jr., Weiner, M., et al. (2010). Docosahexaenoic acid supplementation and cognitive decline in Alzheimer disease: a randomized trial. JAMA *304*, 1903–1911.

Shankar, G.M., Li, S., Mehta, T.H., Garcia-Munoz, A., Shepardson, N.E., Smith, I., Brett, F.M., Farrell, M.A., Rowan, M.J., Lemere, C.A., et al. (2008). Amyloid-β protein dimers isolated directly from Alzheimer's brains impair synaptic plasticity and memory. Nat. Med. *14*, 837–842.

Shimada, H., Ataka, S., Tomiyama, T., Takechi, H., Mori, H., and Miki, T. (2011). Clinical course of patients with familial early-onset Alzheimer's disease potentially lacking senile plaques bearing the E693Δ mutation in amyloid precursor protein. Dement. Geriatr. Cogn. Disord. *32*, 45–54.

Takano, K., Kitao, Y., Tabata, Y., Miura, H., Sato, K., Takuma, K., Yamada, K., Hibino, S., Choshi, T., Iinuma, M., et al. (2007). A dibenzoylmethane derivative protects dopaminergic neurons against both oxidative stress and endoplasmic reticulum stress. Am. J. Physiol. Cell Physiol. *293*, C1884–C1894.

Tomiyama, T., Nagata, T., Shimada, H., Teraoka, R., Fukushima, A., Kanemitsu, H., Takuma, H., Kuwano, R., Imagawa, M., Ataka, S., et al. (2008). A new amyloid β variant favoring oligomerization in Alzheimer's-type dementia. Ann. Neurol. *63*, 377–387.

Tomiyama, T., Matsuyama, S., Iso, H., Umeda, T., Takuma, H., Ohnishi, K., Ishibashi, K., Teraoka, R., Sakama, N., Yamashita, T., et al. (2010). A mouse model of amyloid β oligomers: their contribution to synaptic alteration, abnormal tau phosphorylation, glial activation, and neuronal loss *in vivo*. J. Neurosci. *30*, 4845–4856.

Walsh, D.M., Klyubin, I., Fadeeva, J.V., Cullen, W.K., Anwyl, R., Wolfe, M.S., Rowan, M.J., and Selkoe, D.J. (2002). Naturally secreted oligomers of amyloid β protein potently inhibit hippocampal long-term potentiation *in vivo*. Nature *416*, 535–539.

Yagi, T., Ito, D., Okada, Y., Akamatsu, W., Nihei, Y., Yoshizaki, T., Yamanaka, S., Okano, H., and Suzuki, N. (2011). Modeling familial Alzheimer's disease with induced pluripotent stem cells. Hum. Mol. Genet. *20*, 4530–4539.

The American Journal of Pathology, Vol. 183, No. 1, July 2013

ELSEVIER

The American Journal of
PATHOLOGY

ajp.amjpathol.org

MOLECULAR PATHOGENESIS OF GENETIC AND INHERITED DISEASES

Neurodegenerative Disorder FTDP-17—Related Tau Intron 10 +16C→T Mutation Increases Tau Exon 10 Splicing and Causes Tauopathy in Transgenic Mice

Tomohiro Umeda,*† Takenari Yamashita,* Tetsuya Kimura,‡ Kiyouhisa Ohnishi,* Hiroshi Takuma,* Tomoko Ozeki,§ Akihiko Takashima,‡ Takami Tomiyama,*† and Hiroshi Mori*†

From the Department of Neuroscience, Osaka City University Graduate School of Medicine, Osaka; Core Research for Evolutional Science and Technology,† Japan Science and Technology Agency, Saitama; the Department of Aging Neurobiology,‡ Center for Development of Advanced Medicine for Dementia, National Center for Geriatrics and Gerontology, Obu; and the School of Comprehensive Rehabilitation,§ Osaka Prefecture University, Sakai, Japan*

Accepted for publication March 21, 2013.

Address correspondence to Hiroshi Mori, Ph.D., Department of Neuroscience, Osaka City University Graduate School of Medicine, 1-4-3 Asahimachi, Abeno-ku, Osaka 545-8585, Japan. E-mail: mori@med.osaka-cu.ac.jp.

Frontotemporal dementia and parkinsonism linked to chromosome 17 (FTDP-17) is a neurodegenerative disorder caused by mutations in the tau gene. Many mutations identified in FTDP-17 have been shown to affect tau exon 10 splicing *in vitro*, which presumably causes pathologic imbalances in exon 10^- [3-repeat (3R)] and exon 10^+ [4-repeat (4R)] tau expression and leads to intracellular inclusions of hyperphosphorylated tau in patient brains. However, no reports have investigated this theory using model mice with a tau intronic mutation. Herein, we generated new transgenic mice harboring the tau intron 10 +16C→T mutation. We prepared a transgene construct containing intronic sequences required for exon 10 splicing in the longest tau isoform cDNA. Although mice bearing the construct without the intronic mutation showed normal developmental changes of the tau isoform from 3R tau to equal amounts of 3R and 4R tau, mice with the mutation showed much higher levels of 4R tau at the adult stage. 4R tau was selectively recovered in insoluble brain fractions in their old age. Furthermore, these mice displayed abnormal tau phosphorylation, synapse loss and dysfunction, memory impairment, glial activation, tangle formation, and neuronal loss in an age-dependent manner. These findings provide the first evidence in a mouse model that a tau intronic mutation—induced imbalance of 3R and 4R tau could be a cause of tauopathy. *(Am J Pathol 2013, 183: 211—225; http://dx.doi.org/10.1016/j.ajpath.2013.03.015)*

Frontotemporal dementia and parkinsonism linked to chromosome 17 (FTDP-17) is a neurodegenerative disorder caused by mutations in the tau gene.[1] Its pathologic features include intracellular inclusions of hyperphosphorylated tau aggregates and frontotemporal lobar atrophy. Such tau inclusions are observed not only in FTDP-17 but also in many other neurodegenerative diseases, including Alzheimer disease, which are collectively called tauopathy.[2]

Tau is an axonal microtubule-associated protein and contributes to microtubule stabilization. There are six tau isoforms in humans, the result of alternative splicing of exons 2, 3, and 10 from a single gene. Exon 10 encodes the second of four microtubule-binding domains (MBDs). The alternative splicing of exon 10 generates two types of tau isoforms: exon 10^- mRNA produces 3-repeat (3R) tau with three MBDs, and exon 10^+ mRNA produces 4-repeat (4R) tau with four MBDs. Tau mutations have been identified in exons and introns. Exonic mutations are largely located in or near MBDs and have been shown to attenuate the ability of tau to bind to microtubules,[3,4] enhance tau self-aggregation,[5] and affect exon 10 splicing.[6] All but one intronic mutation is located in the 5′ region of intron 10 and has been shown to affect exon 10 splicing.[7,8] It is known that tau exon 10 splicing is developmentally regulated; in fetal brains, 3R tau is exclusively

Supported by Grants-in-Aid for Scientific Research from the Ministry of Education, Culture, Sports, Science and Technology of Japan (21390271, 21500352, and 23110514); by Grants-in-Aid for Comprehensive Research on Dementia from the Ministry of Health, Labour, and Welfare of Japan; and, in part, by the Alzheimer's Association (IIRG-09-132098).

http://dx.doi.org/10.1016/j.ajpath.2013.03.015

expressed in rodents and humans; however, in adult brains, 4R tau expression becomes exclusive in rodents, whereas 3R and 4R tau are comparably expressed at a ratio of almost 1:1 in humans.[9–11] Thus, mutation-induced alteration of tau exon 10 splicing presumably causes pathologic imbalances in 3R and 4R tau, potentially leading to neurodegeneration. To date, many mouse models of FTDP-17 with tau missense mutations have been generated, but none include a tau intronic mutation.[12,13]

In the present study, we describe a new mouse model of FTDP-17 harboring a tau intron 10 +16C→T mutation and investigated its effects on exon 10 splicing and the onset of pathology *in vivo*. This mutation has been shown to increase tau exon 10 splicing *in vitro*[7,8,14] and cause an accumulation of 4R tau in insoluble fractions in patient brains.[15,16] Herein we show that the mutation indeed increased tau exon 10 splicing in adult mouse brains and subsequently caused abnormal tau phosphorylation, synapse loss and dysfunction, memory impairment, glial activation, tangle formation, and neuronal loss in an age-dependent manner. These findings provide the first evidence in a mouse model that an intronic mutation–induced imbalance in 3R and 4R tau could be a cause of tauopathy even in the absence of a missense sequence.

Materials and Methods

Antibodies

Rabbit polyclonal antibodies reactive to human and mouse tau (pool-2)[11] and specific to human tau (G2)[17] were prepared in our laboratory (Osaka City University Graduate School of Medicine, Osaka, Japan). Mouse monoclonal antibodies to tau phosphorylation at Ser396/Ser404 (PHF-1) and the conformational epitopes of pathologic tau (MC1) were gifts from Dr. Peter Davies (Department of Pathology, Albert Einstein College of Medicine, Bronx, NY). Mouse monoclonal antibodies to tau phosphorylation at Ser202/Thr205 (AT-8; Thermo Scientific, Waltham, MA), the presynaptic marker synaptophysin (SVP-38; Sigma-Aldrich, St. Louis, MO), the mature neuron marker NeuN (Chemicon International, Temecula, CA), the astrocyte marker glial fibrillary acidic protein (GFAP; Cappel, ICN Pharmaceuticals, Aurora, OH), and rabbit polyclonal antibodies to the microglia marker Iba-1 (Wako Pure Chemical Industries, Osaka, Japan) and actin (Sigma-Aldrich) were purchased.

Generation of Transgenic Mice

The transgene for generating transgenic (Tg) mice was prepared from a previously described human tau genomic construct.[18] This construct, tau iEi10, contains the first 18 nucleotides and the last 3.0 kb of tau intron 9 and the first 3.0 kb and the last 38 nucleotides of intron 10 at the corresponding sides of exon 10 in tau441 (the longest tau isoform) cDNA. The intron 10 +16C→T mutation was introduced by site-directed mutagenesis. After the SfiI site in the intron 10 sequence was destroyed by site-directed mutagenesis, tau iEi10 sequences with or without the intronic mutation were ligated into the EcoRV site of the pNN265 vector that contains a 5′ intron and a 3′ intron plus a poly A signal from SV40. This expression carriage was excised from pNN265 with NotI and was inserted into the NotI site of the pMM403 vector that contains the mouse 8.6-kb calcium/calmodulin-dependent kinase IIα promoter to make forebrain-specific transgene expression.[19] Calcium/calmodulin-dependent kinase IIα–tau iEi10 linear sequences were excised from pMM403 with SfiI and injected into B6C3F1 mouse embryos. The obtained Tg mice were backcrossed with C57BL/6 mice for at least 10 generations. All the mice used were heterozygous for the transgene of interest. Expression levels of human tau were determined by Western blot analysis with G2 and pool-2 antibodies. All the animal experiments were approved by the ethics committee of Osaka City University (Osaka, Japan) and were performed in accordance with the Guide for Animal Experimentation, Osaka City University. Every effort was made to minimize the number of animals used and their suffering. The ages and numbers of Tg mice subjected to each assay are summarized in Table 1.

RT-PCR

To examine tau exon 10 splicing in Tg mice, RT-PCR was performed between tau exons 9 and 11. RNA was isolated from brain tissues of the intronic mutant and control Tg mice as well as non-Tg littermates at 7 days and 4 months of age using the SV total RNA isolation kit (Promega, Madison, WI). Reverse transcription and PCR were performed essentially as described previously[7] to separately amplify endogenous mouse tau and transgene-derived human tau. Primer sequences used were as follows: mouse exon 9F, 5′-CACCAAAATCCGGAGAACGA-3′; mouse exon 11R, 5′-CTTTGCTCAGGTCCACCGGC-3′; human exon 9F, 5′-CTCCAAAATCAGGGGATCGC-3′; and human exon 11R, 5′-CCTTGCTCAGGTCAACTGGT-3′. PCR was performed as 30 cycles at 94°C for 30 seconds, at 62°C for 30 seconds, and at 72°C for 45 seconds, with a final 72°C extension for 10 minutes. The expected sizes of PCR products were 390 bp for exon 10^+ mRNA and 297 bp for exon 10^- mRNA for mouse and human tau.

Western Blot Analysis

Mouse brains, not including the hindbrain, were homogenized by sonication in four volumes of 100 mmol/L Tris-HCl, pH 7.6, and 150 mmol/L NaCl Tris-buffered saline (TBS) containing protease inhibitor cocktail (P8340; Sigma-Aldrich). The homogenates were fractionated by three-step ultracentrifugation, including TBS, N-lauroylsarcosinate (sarkosyl), and guanidine hydrochloride (GuHCl) extraction, essentially as described previously.[20] In brief, the homogenates were centrifuged at 100,000 × *g* at 4°C for 15 minutes, and the supernatants were harvested as the TBS-soluble fractions. The